Semiconductor Physics, Quantum Electronics & Optoelectronics. 2002. V. 5, N 1. P. 9-15.

PACS: 78.67. Bf, 78.67.Hc

Urbach's rule peculiarities in structures with CdS_xSe_{1-x} nanocrystals

V.P. Kunets, N.R. Kulish, Vas.P. Kunets, M.P. Lisitsa
Institute of Semiconductor Physics, NAS of Ukraine, 45 prospect Nauky, 03028 Kyiv, Ukraine
Phone: +380 (44) 265 6282

Abstract. We have found that the long wavelength fundamental absorption edge of CdS_xSe_{1-x} nanocrystals grown in an oxide glass follows to the generalized Urbach rule that takes into account both the dynamic (phonon induced) and static (defect induced) disorders of nanocrystal lattice. Temperature intervals with the dominant influence of both disorders on the absorption edge were determined. We have also estimated Urbach rule constants comparing them with the bulk ones. Using various Urbach`s rule theories we analyzed the most considerable changes of nanocrystal parameters when their sizes are decreased down to the quantum scale. It was found that the exciton-phonon coupling constant and exciton localization one are increased; the average electric fields induced by phonons and charged point defects are also increased.

Keywords: Urbach's rule, absorption, nanocrystal, quantum confinement.

Paper received 20.02.02; revised manuscript received 05.03.02; accepted for publication 05.03.02.

1. Introduction

In bulk semiconductors, impurities and defects cause the static disorder of the lattice while phonons induce the dynamic disorder. Both disorders contribute to the tails of the density of states near the main edges of the bands [1,2]. Optical transitions assisted by the tails give rise to the long wavelenth fundamental absorption edge. The near IR luminescence is indicative for the presence of impurities in CdS_XSe_{1-X} nanocrystals [3-5], while the volume CdS-like and CdSe-like LO modes in Raman spectra clearly demonstrate their lattice vibrations [6]. It means that both types of disorders are also present in CdS_XSe_{1-X} NCs inducing similar broadening of their absorption edge. For the first time this effect was pointed out in [7], but it was not studied in detail yet. Therefore, here we report the first detail investigation of the LW absorption edge of CdS_XSe_{1-X} NCs within a wide temperature interval. Two typical cases are considered: $\bar{r} > a_B$ and $\bar{r} < a_B$ (where $\bar{r}$ is the mean radius of NCs and a_B is the Bohr exciton radius in bulk). The findings are analyzed using the most recognized Urbach rule (UR) theories.

2. Samples

The oxide glasses containing CdS_XSe_{1-X} NCs were investigated. Absorption spectra were measured using the standard method with an error less than 5% in the interval 4.2÷500 K. The fixed temperature was kept as a constant with an error less than 2K during the specific measurement. Main NCs parameters were determined by optical methods proposed earlier in [8] (Table 1).

3. Absorption edge spectra

For large NCs ($\bar{r} > a_B$) the absorption coefficient, K, as a function of photon energy $\hbar\omega$, is well described by the ordinary 1/2 degree dependence

$$K = A\left(\hbar\omega - E_g\right)^{1/2} \tag{1}$$

at $\hbar\omega > E_g$, where E_g is the band gap energy, A is a constant (Fig. 1a), while for the small NCs ($\bar{r} < a_B$) it is fitted by the formula

$$K = A\sum_{k=1}^{3}\sum_{\ell n} B_{\ell n}\left(\frac{\mu\bar{r}}{\hbar^2 k_{\ell n}^2}\right)\times \times\left(\frac{2\mu\left(\hbar\omega - E_g - \Delta_{CR}^{k=2,3} - \Delta_{SO}^{k=3}\right)}{\hbar^2 k_{\ell n}^2}\right)^{-3/2} P(u = r/\bar{r}), \tag{2}$$

in the same spectral region. In (2) $k = \varphi_{\ell n}/r$, $\varphi_{\ell n}$ are the roots of the Bessel function, l and n are the orbital and radial quantum numbers, $\Delta_{CR,SO}$ are the crystal field and

Table 1. Parameters of CdS_xSe_{1-x} NCs.

Parameter	$CdS_{0.13}Se_{0.87}$	$CdS_{0.32}Se_{0.68}$	$CdS_{0.64}Se_{0.36}$
Mean radius $\bar{r}$, nm	7.63	2.90	3.00
NC volume, cm^3	1.86×10^{-18}	1.02×10^{-19}	1.13×10^{-19}
Concentration of the lattice atoms, cm^{-3}	1.83×10^{22}	1.29×10^{22}	9.20×10^{21}
Number of atoms in NC	3.41×10^{4}	1.32×10^{3}	1.04×10^{3}
Number of NC atoms per one impurity atom	4.37×10^{3}	2.79×10^{3}	1.38×10^{3}
Number of impurity atoms in NC	7.8	0.47	0.75
Electron effective mass, m_e / m_0	0.140	0.154	0.178
Hole effective mass, m_h / m_0	0.48	0.54	0.61
Low frequency dielectric constant, ε_0	9.56	9.50	9.41
High frequency dielectric constant, ε_∞	5.98	5.81	5.52
Reduced dielectric constant, ε_r	10.39	10.06	9.55

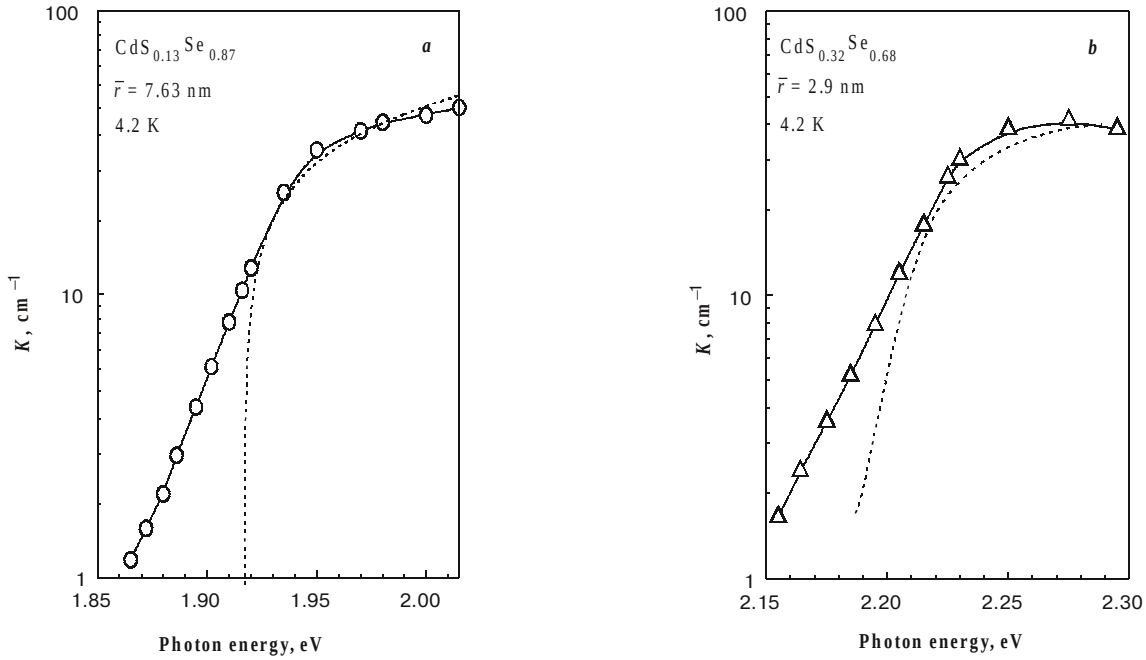

Fig. 1. LW absorption edge of CdS_xSe_{1-x} NCs with $\bar{r} > a_B$ (*a*) and $\bar{r} < a_B$ (*b*).

spin-orbital splittings of the valence band, m is the reduced effective mass, $P(u)$ is the size distribution function, the sum on k = 1, 2, 3 accounts of three valence bands, B_{hn} values describe optical transitions probabilities. According to the formulae (1) and (2) that neglect both aforementioned disorders, the LW edge has to fall down like the dotted lines in Fig. 1, while it falls down exponentially in our experiments even at 4.2 K (solid curves in Fig. 1). That testifies at least about the static disorder of NCs lattice. At high temperatures the edge is additionally broadened by the dynamic disorder of the lattice.

Static lattice disorder

In bulk semiconductors, local changes of E_g are resulted either from the impurities with the different charges and radii or from the non-stoichiometry defects. Thus, a potential relief appears in the real space. The deformed lattice volume around the impurity atom does not exceed two or three coordinate spheres, as a rule. The averaging over a lot of the crystalline cells due to the light absorption at the optical transitions between the levels in the density-of-state tails broadens the edge of the fundamental absorption spectra. In large NCs ($\bar{r} > a_B$, i.e. without confinement effects) the same tails are also formed. Each of the small NCs ($\bar{r} < a_B$, i.e. in the strong confinement regime) can contain either one or a few impurity atoms. Moreover, some of the small NCs can be absolutely pure. Thus, the band gap determined as the distance between the lowest quantum confinement levels will be different even for monodisperse NCs doped with the different number of impurities. In this case, the density-of-state tails (only for the NCs ensemble as a

whole) are formed due to the averaging over the size distribution.

Dynamic lattice disorder

Phonon assisted optical transitions additionally broaden the absorp]tion edge in the bulk crystals and NCs.

4. Urbach's rule peculiarities

From the analysis of the spectra in Fig. 2, we have found that the fan of the absorption lines presented in lgK vs. $\hbar\omega$ coordinates meets the point $(K_0;E_0)$ independently on $\bar{r}$ and X. At low temperatures, the edge is displaced in a parallel manner with the temperature decrease that unambiguously results from the static disorder of NC lattice, while at high temperatures the broadening of the edge is clearly observed demonstrating the dynamic disorder. Thus, the long wavelength absorption edge can be described by the form [1,2]:

$$K = K_0 \exp\left[\frac{\hbar\omega - E_0}{\frac{kT}{\sigma} + W_S}\right] \tag{3}$$

where K_0 and E_0 are the temperature independent constants; W_S describes the broadening of the edge due to the static disorder; $W_d = kT/\sigma$ describes the broadening by the dynamic disorder; and σ depends on the temperature as follows:

$$\sigma = \sigma_0 \left(\frac{2kT}{\hbar\omega_0}\right) \mathrm{th}\left(\frac{\hbar\omega_0}{2kT}\right) \tag{4}$$

Here, σ_0 constant does not depend on temperature; the value of $\hbar\omega_0$ is like the phonon energy $\hbar\omega_{ph}$. Comparing the experimental dependencies $\sigma(T)$ (Fig. 3) with the data calculated by the formula (4) we can estimate $\hbar\omega_0$ and σ_0 (Table 2). From the formula (3), the equation

$$\hbar\omega = E_0 + W_S \ln\left(\frac{K}{K_0}\right) + \frac{\hbar\omega_0 \ln\left(\frac{K}{K_0}\right)}{2\sigma_0 th\left(\frac{\hbar\omega_0}{2kT}\right)} \tag{5}$$

Using W_S estimated above and the equation (7) we have then estimated T_C (Table 2). Figures 2, 3, and 4 testify that the generalized UR is well materialized in CdS_xSe_{1-x}-doped glasses. Table 2 demonstrates the constants obtained from the analysis of the edge. The values of E_g and the exciton energy E_{ex} are presented there, too.

5. Results and discussion

All of the data shows the following changes of the UR constants under transition from bulk to NCs. The constant K_0 is about 3-4 orders of magnitude smaller in NCs than in bulk. The value of E_0 for large NCs ($\bar{r} > a_B$) is similar to that in bulk, but for small NCs ($\bar{r} < a_B$) it is about of the confinement energy greater. The values of $\hbar\omega_0$ are essentially different. In bulk they are similar whatever optical or the acoustic phonon energies are (Table 2) and depend on X [10]. In NCs, they are greater and does not practically depend on $\bar{r}$ and X. Table 2 and Fig. 3 demonstrate considerable differences between σ_0 constants.

To clear up the question about correlations of E_0 and σ_0 values with the CdS_xSe_{1-x} NC parameters, we have analyzed

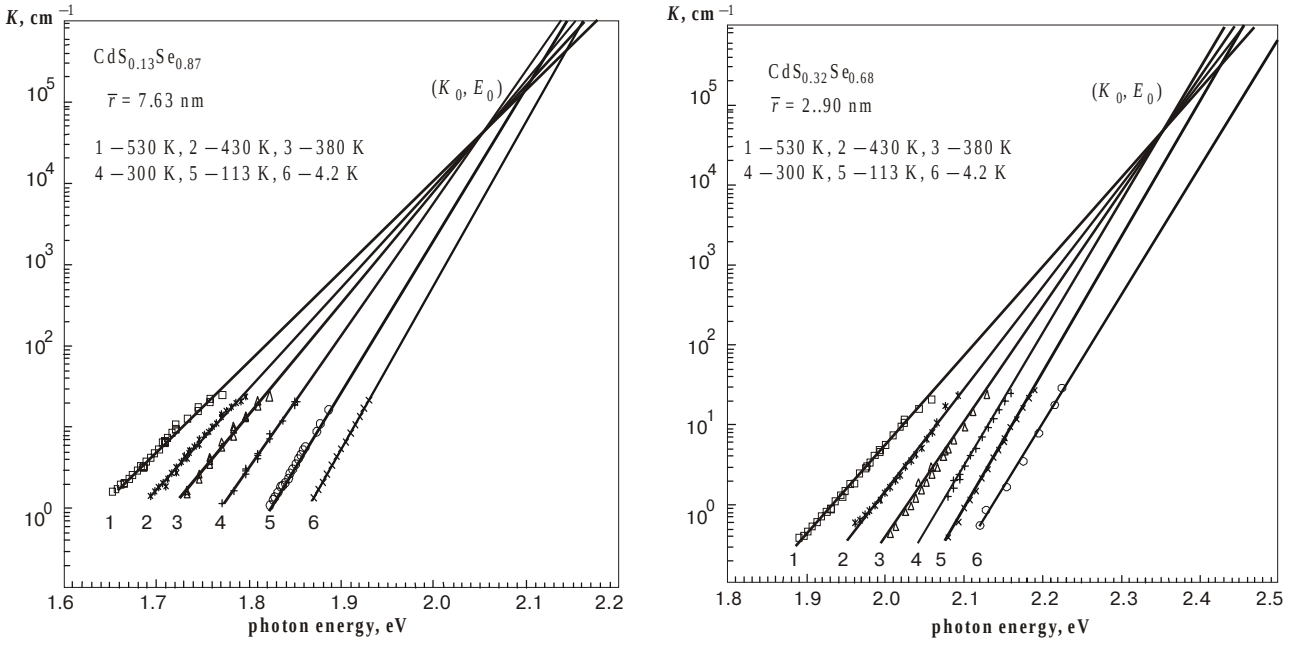

Fig. 2. Typical fans of absorption curves for CdS_xSe_{1-x} NCs at different temperatures.

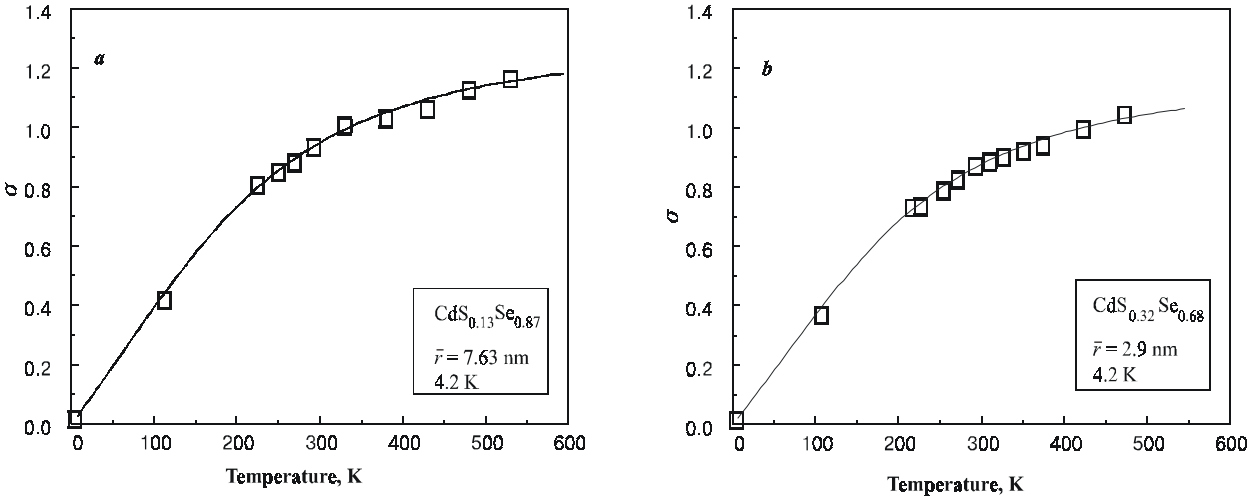

Fig. 3. Temperature dependence of σ parameter.

Table 2. Constants of the Urbach rule.

Parameter	$CdS_{0.13}Se_{0.87}$ bulk	NCs	$CdS_{0.32}Se_{0.68}$ bulk	NCs	$CdS_{0.64}Se_{0.36}$ bulk	NCs	CdS bulk	CdSe bulk
E_g,eV (4.2K)	1.754 (⊥) [9]	1.878	1.842 (⊥) [9]	2.273	2.046 (⊥) [9]	2.456	2.58 (⊥) 2.607(‖)	1.85 (⊥) 1.891 (‖)
E_{ex}, eV(4.2K)	1.736	1.955	1.822	2.273	2.022	2.456	2.5527 (⊥) 2.5840 (‖)	1.825 (⊥) 1.866 (‖)
E_0, eV	2.01 (⊥)[10] 2.00(‖)[10]	2.06	2.15 (⊥) [10] 2.07 (‖) [10]	2.37	2.37 (⊥) [10] 2.28 (‖) [10]	2.527	2.650 (⊥)[10] 2.662 (‖) [10]	1.833 (⊥) [11] 1.862 (‖) [11]
K_0, cm^{-1}	—	$3.63 \cdot 10^4$	—	$7.31 \cdot 10^4$	—	$6.63 \cdot 10^3$	—	$1.5 \cdot 10^7$ (⊥) $2.5 \cdot 10^8$ (‖)
σ_0	2.34 (⊥) [10] 1.98 (‖) [10]	1.30	1.62(⊥) [10] 1.54 (‖) [10]	1.18	1.20 (⊥) [10] 1.13 (‖) [10]	0.94	2.80 (⊥) [10] 2.60 (‖) [10]	2.15 (⊥) [11] 2.50 (‖) [11]
$\hbar\omega_0$, meV	28.5 (⊥) [10] 28.5 (‖) [10]	57	30.6 (⊥) [10] 30.6 (‖) [10]	55	34 (⊥)[10] 34 (‖) [10]	52	38 (⊥) [10] 38 (‖) [10]	21 (⊥) [11] 21 (‖) [11]
$\hbar\omega_{TO}$, cm^{-1} (300K)	—	—	—	—	—	—	242.0(⊥) [12] 235.0 (‖) [12]	171.0(⊥) [12] 168.0(‖) [12]
$\hbar\omega_0$, cm^{-1} (15K)	—	—	—	—	—	—	244.0(⊥) [12] 235.0 (‖) [12]	173.5(⊥) [12] 170.0(‖) [12]
W_s,meV	—	22	—	23	—	27	—	3.4(⊥)(290K) [11] 1.4(‖)(290 K) [11]
T_c,K	—	256	—	267	—	313	—	—
K, cm^{-1} (interval of UR observation)	—	~0.4–7.5	—	~0.4–7.5	—	~0.4-7.5	$5 \div 3 \cdot 10^2$(⊥) $5 \div 3 \cdot 10^2$ (‖)	$3 \cdot 10^1 \div 3 \cdot 10^3$(⊥) $3 \cdot 10^1 \div 3 \cdot 10^3$ (‖)
T,K, (interval of UR observation)	4–300 (⊥) 4–300 (‖)	4–473	4–300 (⊥) 4–300 (‖)	4–473	4–300 (⊥) 4–300 (‖)	4–473	4–300 (⊥) 4–300 (‖)	4–413 (⊥) 4–413 (‖)

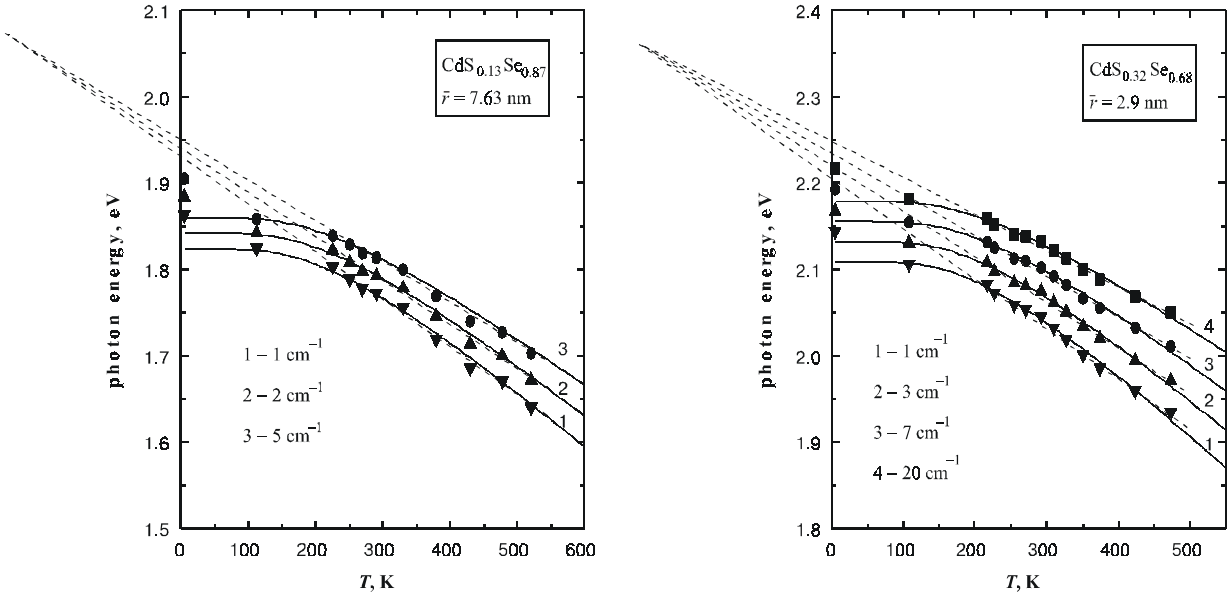

Fig. 4. Typical sets of isoabsorption curves for CdS_xSe_{1-x}-doped glass.

them using the well-known UR theories. Main differences between the models are only concerned with the mechanism of the energy deficit filling up at $\hbar\omega < E_g$. In unalloyed semiconductors this deficit is filled up by phonons. In solid solutions it is satisfied by the local changes of E_g resulted from the local deformations of the crystal potential and electric fields around impurities. All the models can be separated into three groups in accordance with the functional dependencies of E_0 and σ_0 on semiconductor parameters.

Toyozawa's model [13] assumes only the dynamic disorder and exciton-phonon filling mechanism of the energy photon deficit at $\hbar\omega < E_g$. In this case,

$$E_0 = E_{ex} + \frac{(\hbar\alpha_0)^2}{4m_{ex}}, \tag{8}$$

$$\sigma_0 = 2/3G, \tag{9}$$

where E_{ex} is the exciton energy in absorption spectra at 4.2 K; $m_{ex} = m_e + m_h$ is the exciton translational mass; $m_e(m_h)$ is the electron (hole) effective mass; α_0 describes the exciton localization; G is the exciton-phonon coupling constant.

In Redfield's model [14, 15] the energy deficit is provided by the electron tunneling forcing by the local electric field near the point charged defects or due to LO phonons. The average value of the field induced by LO phonons can be estimated by the formula:

$$F_{rms} = \sqrt{\left\langle F^2 \right\rangle} = \\ = (2\varepsilon_0\hbar\omega_0)\left(\sqrt{3}\varepsilon^* e a_{ex}\pi\right)^{-1} \coth\left(\hbar\omega_0/2kT\right), \tag{10}$$

where $\varepsilon^* = 1/\varepsilon_0 + 1/\varepsilon_\infty$, ε_0 and $\varepsilon\mu$ are the low and high frequency dielectric constants. In this model, E_0 is associated with E_g at $T = 0$ K while σ_0 is given by:

$$\sigma_0 = C\sqrt{3}\varepsilon^* a_{ex}\pi / 4\varepsilon_0 \tag{11}$$

where C is a constant.

Bonch-Bruevich's model [16] takes into account only the static disorder that smoothes the potential relief. The latter is characterized by the so-called optimal fluctuations, and the absorption edge spectra is given by:

$$K = K_0 \exp\left(\frac{\hbar\omega - E_0}{W_S}\right). \tag{12}$$

The strength of the electric fluctuated field is written through W_S as follows:

$$E_S = \frac{1}{e}\sqrt{\frac{36m_e}{\hbar^2}W_S^3} \tag{13}$$

In the case when the potential relief is formed by the point charged defects, W_S depends on their concentration N_t as follows [16]:

$$W_S = 2.2E_B\left(N_t a_{ex}^3\right)^{0.4}, \tag{14}$$

where $E_B = e^2/2\varepsilon_r a_{ex}$, and e_r is the reduced dielectric constant.

We have used these models to analyze the influence of NC sizes on the UR parameters (Table 3). CdS_xSe_{1-x} NCs are chaotically oriented in a glass. Therefore, the long wavelength edge is formed by transitions in $\vec{E} \perp C$ polarization and NC parameters can be compared with the bulk constants corresponding to the component $\vec{E} \perp C$. Analyzing the data listed in Table 3, we have revealed the following peculiarities.

Table 3. NC parameters obtained from the UR analysis

	$CdS_{0.13}Se_{0.87}$		$CdS_{0.32}Se_{0.68}$		$CdS_{0.64}Se_{0.36}$		CdS	CdSe
parameter	NCs	bulk (⊥)	NCs	bulk (⊥)	NCs	bulk (⊥)	bulk (⊥)	bulk
G	0.51	0.28	0.56	0.41	0.71	0.56	0.24	0.31
α_0, cm^{-1}	$8.01 \cdot 10^6$	$7.46 \cdot 10^6$	$1.98 \cdot 10^7$	$1.08 \cdot 10^7$	$1.81 \cdot 10^7$	$1.63 \cdot 10^7$	$2.26 \cdot 10^7$	$5.20 \cdot 10^6$
N_t, cm^{-3}	$4.19 \cdot 10^{18}$	—	$4.63 \cdot 10^{18}$	—	$6.65 \cdot 10^{18}$	—	—	$4.00 \cdot 10^{16}$ [1)]
N_M, cm^{-3}	$3.52 \cdot 10^{17}$	—	$5.14 \cdot 10^{17}$	—	$9.31 \cdot 10^{17}$	—	$1.74 \cdot 10^{18}$	$2.65 \cdot 10^{17}$
$\hbar\omega_f$, meV	57	28.5	55	30.6	52	34	38	21
F_{rms}, V/cm	$1.74 \cdot 10^6$	$7.75 \cdot 10^5$	$1.96 \cdot 10^6$	$1.02 \cdot 10^6$	$1.91 \cdot 10^6$	$1.42 \cdot 10^6$	$1.88 \cdot 10^6$	$6.10 \cdot 10^5$
F_S, V/cm	$2.80 \cdot 10^5$	—	$3.13 \cdot 10^5$	—	$4.29 \cdot 10^5$	—	—	$1.38 \cdot 10^4$

[1)] at $T = 290$ K

(a) The exciton localization is increased in NCs. It is obvious because the exciton is confined by the NC surface *a priori*.

(b) The exciton-phonon coupling constant is increased.

(c) The most probable source of the absorption edge broadening in the bulk is the shallow donor-like defects. In NCs their relative concentration N_t is greater because NCs are synthesized in an oxide multicomponent matrix that contains a lot of "potential" impurities. According to Mott criterion

$$a_B (N_M)^{1/3} \geq 0.25, \qquad (15)$$

where N_M is the critical concentration which is necessary for the impurity band appearance to start. In CdS_xSe_{1-x}, NCs N_t exceeds greatly the critical value which results in the impurity band growth in bulk. It means that the carriers are not frozen and N_t does not depend on temperature, i. e., the absorption edge broadening does not depend on temperature in the cryogenic region, too. In bulk CdSe $N_t < N_M$ and the carriers are frozen. As a result N_t is decreased with the temperature decrease, i. e., W_S is decreased [1]. Using the value of N_t we have then estimated a number of NC atoms corresponding to a single impurity atom in it (Table 1).

For example, one CdS_xSe_{1-x} NC with $\bar{r}$ =7.63 nm contains about 8 impuriy atoms while at $\bar{r}$ =3.00 nm, it contains less then one similar atom, i.e. at $\bar{r}$ =3.00 nm, there are some quantity of non-doped NCs in glass.

(d) The electric field induced by the point charged defects is risen in NC because of their greater relative concentration in comparison with the bulk one.

(e) Some exceeding of the phonon induced electric field F_{rms} in comparison with the bulk one seems to be related to the polarization effects in a glass matrix and hydrostatic glass pressure.

The conclusion that the LW absorption edge of CdS_xSe_{1-x} NCs is described by the generalized UR is supported: (a) by the meeting in a single point of the absorption curves for fans presented in lgK vs. $\hbar\omega$ coordinates; (b) by the typical temperature dependence of σ parameter; (c) by the typical behavior of the isoabsorption curves for the simultaneous effects of both the static and dynamic disorders of the lattice (see Fig. 4). All the peculiarities of UR constants can be explained as follows.

Decreasing of K_0 is related to the small fraction volume of CdS_xSe_{1-x} compound in an oxide matrix (~0.1%). The greater value of E_0 in small NCs ($\bar{r} < a_B$) results from the quantum confinement of exciton motion. In bulk CdS_xSe_{1-x} solid solution, σ_0 depends on X [10] being resulted from the structural disorder at the relative increasing one of the anion component that induces exciton localization effects. In CdS_xSe_{1-x}, NC excitons are greater localized *a priori*, which correlates with further lowering σ_0 and lead to the exciton-phonon coupling constant increasing. In NCs, the value of $\hbar\omega_0$ constant exceeds that of the bulk. It seems reasonable to be explained by broadening the edge due to additional effects of both glass matrix phonons and surface NCs phonons. The role of the static disorder (W_S constant) was estimated for CdS_xSe_{1-x} NCs for the first time. Its high value in NCs results from their relatively high doping level by the charged point impurities. Finally, characteristic temperature T_C corresponding to the equal contributions of the static and dynamic disorders was determined, and the electric fields induced by both types of the disorders were estimated.

6. Conclusion

The LW absorption edge of CdS_xSe_{1-x} NCs is well described by the generalized UR. All the aforementioned UR models have to be defined more precisely because of the following. The potential relief induced only by a single impurity atom in NC can not be considered as the smoothed one. It is also not clear yet how such potential can be introduced for the structure with the size dispersion. The confinement effect on the phonon spectra as well as on the exciton motion should be taken into account in the theories. Then, the effect of the NC surface on the phonon induced electric field is not yet sufficiently understood. All of these items do not obviously break the UR complicating only its analysis. Their accounting will allow to determ more

precisely the correlation between the UR constants and NC parameters and may be to observe new peculiarities in future.

Acknowledgments

The authors thank to Malysh N.I. for his assistance in measurements.

References

1. B.I. Shklovsky, A.L. Efros. *Electronic properties of doped semiconductors* (in Russian), Nauka, Moscow (1979).
2. V. Sa-Yakanit, N.R. Glyde. Urbach tails and disorder // *Comments Matter Phys*. 13(1), pp. 35-48 (1987).
3. A.I. Ekimov, I.A. Kudryavtsev, M.G. Ivanov, Al.L. Efros. Photoluminescence of quasi-zero-dimensional semiconductor structures (in Russian) // *Fizika tverdogo tela* . 31(8), pp. 192-207 (1989).
4. I.B. Ermolovich, N.R. Kulish, V.P. Kunets, M.P. Lisitsa, N.I. Malysh, M.K. Sheinkman. Quantum confinement effects in absorption impurity-defect luminescence spectra of CdSSe-doped glasses (in Russian) // *Optika i spektroskopiya* 64(4), pp. 855-859 (1990).
5. M.Ya. Valakh, N.R. Kulish, V.P. Kunets, M.P. Lisitsa, G.Yu. Rudko. Nature of radiative recombination in quasi-zero-dimensional CdS_XSe_{1-X} crystals (in Russian) // *Ukrainian Phys. Journal* 38(11), pp. 1667-1672 (1993).
6. V.P. Kunets, N.R. Kulish, M.P. Lisitsa, A. Mlayah, M.Ya Valakh. Size effects in TEM investigations, absorption and Raman scattering spectra of CdSSe nanocrystals embedded into glass matrices (in Russian) // *Ukrainian Phys. Journal* 45(2), pp. 164-167 (2000).
7. N.R. Kulish, V.P. Kunets, M.P. Lisitsa. Absorption spectra of semiconductor microcrystals under the quantum confinement (in Russian) // *Ukrainian Phys. Journal* 35(12), pp. 1817-1821 (1990).
8. N.R. Kulish, V.P. Kunets, M.P. Lisitsa. Determination of semiconductor quantum dots parameters by optical methods // *Superlattices and Microstructures* 22(3), pp. 341-351 (1997).
9. G.S. Park, D.C. Reynolds. Exciton structure in photoconductivity of CdS, CdSe and CdS:Se single crystals // *Phys. Rev*. 132(6), pp. 2450-2454 (1963).
10. L. Samuel, Y. Brada, R. Besserman. Fundamental absorption edge in mixed single crystals of II-VI compounds // *Phys. Rev.* B. 37(9), pp. 4671-4677 (1988).
11. M.P. Lisitsa, N.I. Kulish, N.I. Malysh, B.M. Bulakh. Fundamental absorption edge of CdSe at high excitation levels (in Russian) // *Fizika i tekhnika poluprovodnikov* 19(8), pp. 1399-1404 (1985).
12. H.W. Verleur, A.S. Barker. Optical phonons in mixed crystals of $CdSe_YS_{1-Y}$ // *Phys. Rev*. 155(3), pp. 750-763 (1975).
13. Y. Toyozawa. The Urbach rule and exciton-lattice interaction // *Techn. Report. ISSP* A(119), pp. 1-68 (1964).
14. D. Redfield. Electric fields of defects in solids // *Phys. Rev*. 130(3), pp. 914-915 (1963).
15. J. D. Dow, D. Redfield. Urbach rule // *Phys. Rev. B*. 5(2), pp. 594-599 (1972).
16. V.L. Bonch-Bruevich, I.P Zvyagin, R. Kaiper et. al. *Electronic theory of disordered semiconductors* (in Russian), Nauka, Moscow (1981).